

Spin-Density Maps for an Oxamido-Bridged Mn(II)Cu(II) Binuclear Compound. Polarized Neutron Diffraction and Theoretical Studies

Valery Baron,[†] Béatrice Gillon,^{*,†} Olivier Plantevin,[†] Alain Cousson,[†] Corine Mathonière,[‡] Olivier Kahn,^{*,‡} André Grand,[§] Lars Öhrström,[§] and Bernard Delley[⊥]

Contribution from the Laboratoire Léon Brillouin, Centre d'Etudes Nucléaires de Saclay, 91191 Gif sur Yvette, France, Laboratoire des Sciences Moléculaires, Institut de Chimie de la Matière Condensée de Bordeaux, UPR CNRS No. 9048, 33608 Pessac, France, Laboratoire de Chimie de Coordination, URA CNRS No. 1195, Centre d'Etudes Nucléaires de Grenoble, 38054 Grenoble, France, and Paul Scherrer Institute Zürich, Badenerstrasse 569, 8048 Zürich, Switzerland

Received May 8, 1996[⊗]

Abstract: This paper is devoted to the determination of the spin density in the $S = 2$ ground state of $[\text{Mn}(\text{Me}_6\text{-[14]ane-N}_4)\text{Cu}(\text{oxpn})](\text{CF}_3\text{SO}_3)_2$ with $\text{Me}_6\text{-[14]ane-N}_4 = (\pm)\text{-5,7,7,12,14,14-hexamethyl-1,4,8,11-tetraazacyclotetradecane}$ and $\text{oxpn} = N,N'\text{-bis(3-aminopropyl)oxamido}$. The crystal structure, previously determined at room temperature through X-ray diffraction and at 40 K through unpolarized neutron diffraction, consists of oxamido-bridged $[\text{Mn}(\text{Me}_6\text{-[14]ane-N}_4)\text{Cu}(\text{oxpn})]^{2+}$ cations and non-coordinated triflate anions. Within the cation the $S_{\text{Mn}} = 5/2$ and $S_{\text{Cu}} = 1/2$ local ground states are antiferromagnetically coupled, which gives rise to a ground $S = 2$ and an excited $S = 3$ pair states, with a quintet–septet energy gap of -93.3 cm^{-1} . The experimental spin density has been deduced from polarized neutron diffraction data recorded at 2 K under 50 kOe. Positive spin populations were observed on the manganese side, and negative spin populations on the copper side. The delocalization of the spin density from the metal center toward the terminal and bridging ligands was found to be more pronounced on the copper side than on the manganese side, and the nodal surface (of zero spin density) is closer to the manganese than to the copper atom. The experimental data have been compared to the results of several theoretical approaches, corresponding to different levels of sophistication. These approaches are as follows: (i) the pure Heitler–London description of the $S = 2$ ground state; (ii) the incorporation of the spin delocalization in the Heitler–London scheme, using the concept of magnetic orbitals in the extended Hückel formalism; and (iii) two types of density functional theory methods. In cases ii and iii, the experimental spin populations have been fairly well reproduced. The DFT approaches have provided some important insights on both spin-delocalization and spin-polarization effects.

Introduction

Molecular magnetism is a field of research dealing with the chemistry and the physics of open-shell molecules and molecular assemblies containing open-shell units.¹ The spin carriers may be transition metal ions as well as purely organic radicals.

Among all the molecules relevant to molecular magnetism, those containing two (or possibly more) kinds of metal ions have played a particularly important role. Two reasons, at least, justify this situation. First, the diversity of situations which can be encountered concerning the interaction between two spin carriers **A** and **B** within a molecular unit is much greater when **A** and **B** are different. For instance, the strict orthogonality of the magnetic orbitals leading to the stabilization of the molecular state of highest spin is much easier to achieve in heterobimetallic species.² Secondly, with several kinds of magnetic centers it is possible to design lattices showing quite peculiar spin topologies, for instance ferrimagnetic one-, two-, or three-dimensional lattices.^{3,4}

One of the very active facets of molecular magnetism concerns the design and the synthesis of compounds exhibiting a spontaneous magnetization below a critical temperature. The very first compounds of that kind were reported in 1986.^{5,6} The majority of molecular-based magnets reported so far are heterobimetallic species, in which different metal ions are bridged by extended bisbidentate ligands such as oxamato,^{7–12} oxamido,^{13,14} oxalato,^{15–19} dithiooxalato,²⁰ or oximato.^{21,22} The interaction between nearest neighbor spin carriers may be ferromagnetic; it may be antiferromagnetic as well with a noncompensation of the local spins. In this latter case, the most favorable situation is that where the difference between the local spins $|S_{\text{A}} - S_{\text{B}}|$ is the largest, which is realized in Mn(II)Cu(II) compounds with $S_{\text{Mn}} = 5/2$ and $S_{\text{Cu}} = 1/2$ local spins. The

(5) Miller, J. S.; Calabrese, J. C.; Epstein, A. J.; Bigelow, R. W.; Zang, J. H.; Reiff, W. M. *J. Chem. Soc., Chem. Commun.* **1986**, 1026.

(6) Pei, Y.; Verdaguer, M.; Kahn, O.; Sletten, J.; Renard, J. P. *J. Am. Chem. Soc.* **1986**, *108*, 428.

(7) Kahn, O.; Pei, Y.; Verdaguer, M.; Renard, J. P.; Sletten, J. *J. Am. Chem. Soc.* **1988**, *110*, 782.

(8) Nakatani, K.; Bergerat, P.; Codjovi, E.; Mathonière, C.; Pei, Y.; Kahn, O. *Inorg. Chem.* **1991**, *30*, 3977.

(9) Stumpf, H. O.; Pei, Y.; Kahn, O.; Sletten, J.; Renard, J. P. *J. Am. Chem. Soc.* **1993**, *115*, 6738.

(10) Stumpf, H. O.; Ouahab, L.; Pei, Y.; Grandjean, D.; Kahn, O. *Science* **1993**, *261*, 447.

(11) Stumpf, H. O.; Ouahab, L.; Pei, Y.; Bergerat, P.; Kahn, O. *J. Am. Chem. Soc.* **1994**, *116*, 3866.

(12) Stumpf, H. O.; Pei, Y.; Michaut, C.; Kahn, O.; Renard, J. P.; Ouahab, L. *Chem. Mater.* **1994**, *6*, 257.

[†] Centre d'Etudes Nucléaires de Saclay.

[‡] Institut de Chimie de la Matière Condensée de Bordeaux.

[§] Centre d'Etudes Nucléaires de Grenoble.

[⊥] Paul Scherrer Institute Zürich.

[⊗] Abstract published in *Advance ACS Abstracts*, November 15, 1996.

(1) Kahn, O. *Molecular Magnetism*; VCH: New York, 1993.

(2) Kahn, O.; Galy, J.; Journaux, Y.; Jaud, J.; Morgenstern-Badarau, I. *J. Am. Chem. Soc.* **1982**, *104*, 2165.

(3) Kahn, O. *Struct. Bonding (Berlin)* **1987**, *68*, 89.

(4) Kahn, O. *Adv. Inorg. Chem.* **1995**, *43*, 179.

first molecular-based heterobimetallic magnets have been oxamato- and oxamido-bridged Mn(II)Cu(II) species.^{7–14} Therefore, it was worthwhile to analyze the interaction between Mn(II) and Cu(II) ions through such an extended bridge in a thorough fashion. Polarized neutron diffraction is a unique tool for that. This technique permits the whole spin density distribution for a molecule in the solid state to be obtained. Because neutron spin interacts with the unpaired electronic spins in matter, the study of magnetic neutron diffraction provides direct information on the unpaired electron distribution in a material. The polarized neutron diffraction technique is moreover particularly sensitive for investigating very weak magnetism, for instance in purely organic magnetic molecular materials, where only one unpaired electron per molecule is responsible for magnetism.

This technique is nowadays more and more applied to the field of molecular magnetism. One of the first applications in this domain dealt with paramagnetic organic free radicals.²³ Recent studies of ferromagnetic nitronyl nitroxide radicals have permitted the analysis of the magnetic interaction pathway between the magnetic centers through the unsaturated organic skeleton.²⁴ To the best of our knowledge only two bimetallic species have been investigated by polarized neutron diffraction until now, namely a binuclear copper(II) compound in which the Cu(II) ions are ferromagnetically coupled through two hydroxo bridges,²⁵ and a Cu(II)Ni(II) heterobinuclear compound in which the Cu(II) and Ni(II) ions are antiferromagnetically coupled through two phenolic oxygen atoms, resulting in a spin doublet ground state.²⁶ The determination of the detailed induced spin density map has allowed evidence for positive spin delocalization toward the bridging oxygen atoms for the former compound to be obtained. In contrast, the antiferromagnetic coupling leads to a compensation of the spin densities of opposite signs on the bridges for the latter compound.

In this paper, we focus on the simplest case of Mn(II)Cu(II) heterobimetallics, i.e. a binuclear species. The compound we selected is [Mn(Me₆-[14]ane-N₄)Cu(oxpn)](CF₃SO₃)₂, with Me₆-[14]ane-N₄ = (±)-5,7,7,12,14,14-hexamethyl-1,4,8,11-tetraazacyclotetradecane and oxpn = *N,N'*-bis(3-aminopropyl)oxamido. The crystal structure and the magnetic and optical properties of this compound hereafter abbreviated as MnCu have already been described.²⁷ The interaction between the $S_{Mn} = 5/2$ and

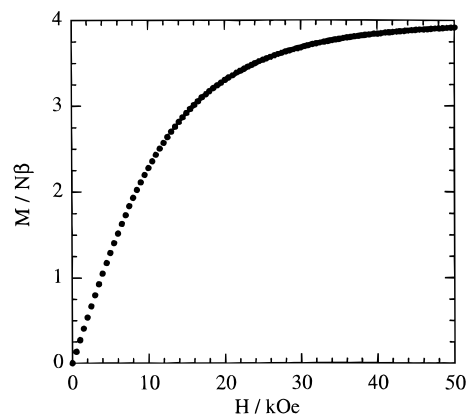


Figure 1. Field dependence of the magnetization for MnCu at 2 K.

$S_{Cu} = 1/2$ local states gives rise to $S = 2$ and 3 pair states. The energy gap between ground quintet and excited septet states has been found as $3J = -93.9 \text{ cm}^{-1}$. It is worth remembering that the magnitude of the intramolecular antiferromagnetic interaction has been determined from the temperature dependence of both the molar magnetic susceptibility χ_M and the optical absorption spectrum. Below ca. 40 K, the $S = 3$ excited state is essentially depopulated. Moreover the zero-field splitting within the $S = 2$ ground state is very weak. It follows that in the 2–40 K temperature range the magnetic susceptibility follows the Curie law $\chi_M T = 2.94 \text{ cm}^3 \text{ K mol}^{-1}$.

The paper is organized as follows: The first part is devoted to the presentation of the polarized neutron diffraction experiment, together with the spin density maps deduced from the neutron data. The second part is devoted to the theoretical discussion of the findings, using different methods corresponding to different levels of sophistication. Finally, in a conclusion, the perspectives of the polarized neutron diffraction technique in the area of molecular magnetism are emphasized.

Experimental and Computational Methods

Synthesis. [Mn(Me₆-[14]ane-N₄)Cu(oxpn)](CF₃SO₃)₂ was synthesized as previously described.²⁷ Well-shaped single crystals as large as 56 mm³ were obtained by aerial diffusion of diethyl oxide into a solution of MnCu in acetonitrile.

Magnetization. The field dependence of the magnetization was measured at 2 K with a Quantum Design MPMS-5S SQUID magnetometer working up to 50 kOe. The curve is shown in Figure 1. This curve within the errors follows the Brillouin function expected for a $S = 2$ state with the Zeeman factor $g_2 = 2.00$.

Low-Temperature Structure Determination through X-ray and Neutron Diffraction. The crystal structure of MnCu was already known from an X-ray diffraction study at room temperature.²⁷ This structure is recalled in Figure 2. However, the hydrogen positions were not refined. Combined studies of neutron diffraction at 40 K and X-ray diffraction at 25 K were performed in order to determine the precise nuclear structure, in particular the hydrogen positions and the thermal parameters. These pieces of information are necessary for the polarized neutron data treatment. The positional and thermal parameters are not expected to vary significantly in the low-temperature range, below 40 K. The details of the low-temperature structure will be presented elsewhere.²⁸ We restrict ourselves here to comparing the values of the lattice parameters at room temperature and 40 K in Table 1.

Polarized Neutron Experiment. The experimental work was performed on the polarized neutron diffractometer 5C1 of the L.L.B. at the Orphee reactor in Saclay. A Heusler monochromator was used to obtain a polarized neutron beam, with a beam polarization equal to 0.920(4). The information relative to the polarized neutron data collection is reported in Table 2. Three data collections were performed at 2 K with an applied magnetic field of 50 kOe, on two different samples. In order to avoid multiple scattering problems arising from

(13) Pei, Y.; Kahn, O.; Nakatani, K.; Codjovi, E.; Mathonière, C.; Sletten, J. *J. Am. Chem. Soc.* **1991**, *113*, 6558.

(14) Nakatani, K.; Carriat, J. Y.; Journaux, Y.; Kahn, O.; Lloret, F.; Renard, J. P.; Pei, Y.; Sletten, J.; Verdager, M. *J. Am. Chem. Soc.* **1989**, *111*, 5739.

(15) Zhong, Z. J.; Matsumoto, H.; Okawa, H.; Kida, S. *Chem. Lett.* **1990**, 87.

(16) Tamaki, H.; Zhong, Z. J.; Matsumoto, N.; Kida, S.; Koikawa, M.; Achiwa, N.; Hashimoto, Y.; Okawa, H. *J. Am. Chem. Soc.* **1992**, *114*, 6974.

(17) Decurtins, S.; Schmalke, H. W.; Oswald, H. R.; Linden, A.; Ensling, J.; Gülich, P.; Hauser, A. *Inorg. Chim. Acta* **1994**, *216*, 65.

(18) Okawa, H.; Mitsumi, M.; Ohba, M.; Koda, M.; Matsumoto, N. *Bull. Chem. Soc. Jpn.* **1994**, *67*, 2139.

(19) Mathonière, C.; Nuttall, C. J.; Carling, S. G.; Day, P. *Inorg. Chem.* **1996**, *35*, 1201.

(20) Tamaki, H.; Mitsumi, M.; Nakamura, K.; Matsumoto, N.; Kida, S.; Okawa, H.; Iijima, S. *Chem. Lett.* **1992**, 1975.

(21) Lloret, F.; Ruiz, R.; Julve, M.; Faus, J.; Journaux, Y.; Castro, I.; Verdager, M. *Chem. Mater.* **1992**, *4*, 1150.

(22) Lloret, F.; Ruiz, R.; Cervera, B.; Castro, I.; Julve, M.; Faus, J.; Real, A.; Sapina, F.; Journaux, Y.; Colin, J. C.; Verdager, M. *J. Chem. Soc., Chem. Commun.* **1994**, 2615.

(23) Brown, P. J.; Capiomont, A.; Gillon, B.; Schweizer, J. *J. Magn. Mater.* **1979**, *14*, 289.

(24) Zheludev, A.; Bonnet, M.; Ressouche, E.; Schweizer, J.; Wan, M.; Wang, H. *J. Magn. Mater.* **1994**, *135*, 147.

(25) Figgis, B. N.; Mason, R.; Smith, A. R. P.; Varghese, J. N.; Williams, G. A. *J. Chem. Soc., Dalton Trans.* **1983**, 703.

(26) Gillon, B.; Cavata, C.; Schweiss, P.; Journaux, Y.; Kahn, O.; Schneider, D. *J. Am. Chem. Soc.* **1989**, *111*, 7124.

(27) Mathonière, C.; Kahn, O.; Daran, J. C.; Hilbig, H.; Köhler, F. H. *Inorg. Chem.* **1993**, *32*, 4057.

(28) Baron, V.; Gillon, B.; Kahn, O.; Rundhöf, H.; Tellgren, R. To be submitted for publication.

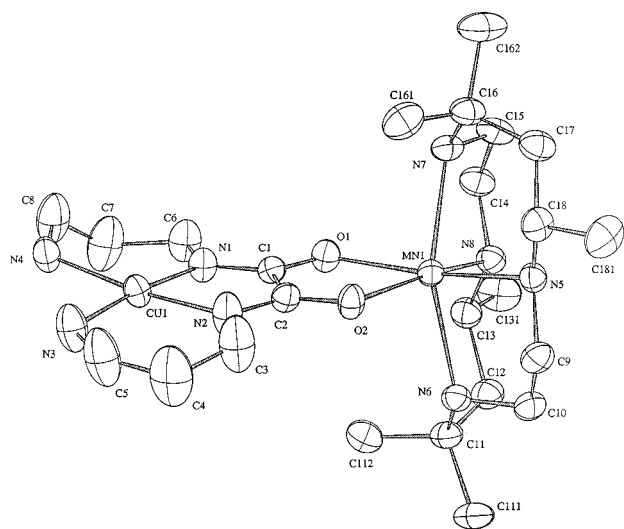


Figure 2. Molecular structure with the atom labeling for the binuclear cation in MnCu.

Table 1. Cell Parameters at 298 and 40 K

cell parameters	$T = 298$ K	$T = 40$ K
a (Å)	17.781	17.525(3)
b (Å)	18.202	17.955(4)
c (Å)	12.893	12.804(2)
β (deg)	105.48	104.97(2)

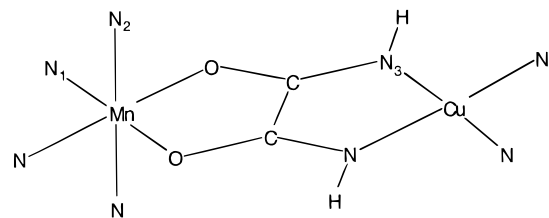
Table 2. Experimental Data Concerning the Polarized Neutron Measurements

monochromator	Cu ₂ MnAl (110)		
wavelength (Å)	0.83		
beam polarisation	0.920(4)		
flipping efficiency	1		
T (K)	2		
H (T)	5		
crystal size (mm ³)	13.5		56
vertical axis	a	b	b
no. of reflcns	216	26	68

weak nuclear reflections, only reflections with $|F_N| > 10^{-12}$ cm were measured. On the first crystal of size 13.5 mm³, two sets of data were collected with two different experimental geometries; the a and b crystal axes were set along the vertical direction, successively. The flipping ratio measurements with a vertical provided 236 (hkl) independent reflections with $h = 0$ to 5. The second set with b vertical consisting of 27 reflections was completed by the subsequent measurement of 69 reflections on a larger single crystal of 56 mm³. These data include the reflections with $k = 0$ to 3. Among the 332 measured reflections, 297 were inequivalent, and 35 were common to at least two sets of data. The flipping ratios were corrected for imperfect beam polarization. A correction for polarization of the hydrogen nuclear spins was performed on the magnetic structure factors. At 2 K and under a high magnetic field the hydrogen nuclear spin polarization, $f_{\text{HNP}}^{\text{H}}$, was estimated as 0.003722×10^{-12} cm. The uncertainty on the nuclear structure factors was not taken into account in the estimation of the errors on the magnetic structure factors.

Magnetic Orbital Calculations. These were performed by using the extended Hückel formalism without charge iteration. For the sake of simplicity the actual geometry of MnCu was somewhat simplified. The Me₆[14]ane-N₆ ligand was replaced by four ammonia molecules, and the oxpn ligand was replaced by an unsubstituted [O₂C₂(NH)₂]²⁻ group and two ammonia molecules. The lone pairs of the NH₃ ligands were described by a spherical atomic orbital. The parametrization utilized was the following: Mn, 4s (1.80, -9.75 eV), 4p (1.80, -5.89 eV), 3d (5.15, coeff. 0.53108, 1.90, coeff. 0.64788, -11.67 eV); Cu, 4s (2.20, -11.40 eV), 4p (2.20, -6.06 eV), 3d (5.96, coeff. 0.59332, 2.30, coeff. 0.57442, -14.00 eV); C, 2s (1.625, -21.4 eV), 2p (1.625, -11.40 eV); N, 2s (1.95, -26.00 eV), 2p (1.95, -13.40 eV); O, 2s (2.275, -32.30 eV), 2p (2.275, -14.80 eV); N(H₃) lone pair (1.95,

-19.20 eV). The skeleton of the hypothetical binuclear compound is schematized below:



Density Functional Theory Calculations. Density functional theory (DFT) has recently been shown to give spin populations in good agreement with experimental data for organic radicals.^{29–31} In this study two types of DFT computations were performed. In the former approach the DGauss DFT program included in the UniChem package from Cray Research Inc. was used.^{32,33} At the local spin density level the functional of Vosko, Wilk, and Nusair (VWN) was utilized.³⁴ For the non-local corrections to the exchange-correlation energy the Becke–Perdew (BP) functional³⁵ including a gradient corrected exchange was used in a perturbative way on the LSD-SCF density. The incorporation of this correction self-consistently should in principle be more correct, but it also considerably increases the computational effort. A few test calculations were performed in order to investigate this effect. The DGauss program uses Gaussian basis sets optimized for LSD calculations. We used a double- ζ split-valence plus polarization basis set, DZVP,³⁸ that has recently been used with satisfactory results.^{36,37} The contracted basis sets had the following composition: H [2s]; C, N, O [3s, 2p, 1d]; Cu, Mn [5s, 3p, 2d]. The corresponding DZVP2 basis (with two polarization functions) as well as the TZVP (H, C, N, O) + DZVP2 (Cu, Mn) basis set were used in some test calculations, but showed only small differences in spin populations as compared to the DZVP basis set. Earlier studies are not conclusive as for the importance of including the non-local corrections in every SCF iteration.^{39,40} In our case this gave no phenomenological differences, although we noted a small general increase in the spin polarization. On the contrary, the spin transfer from manganese to the ligands decreased somewhat whereas no corresponding effect was detected at the copper atom. Therefore, as a reasonable compromise, we used the DZVP basis with the perturbative non-local corrections, and all the reported results have been computed with this method. We also have to deal with the fact that the $S = 2$ ground state of the compound cannot be correctly described by a single determinant DFT wave function since this is not the highest spin state. We instead computed the so-called broken symmetry (BS) state, where the positive and negative spin densities have been centered on manganese and copper atoms, respectively. This approximation may be corrected by using the approach of Noodleman.⁴¹ The energy difference between the $S = 3$ high-spin (HS) and BS states

(29) Zheludev, A.; Barone, V.; Bonnet, M.; Delley, B.; Grand, A.; Ressouche, E.; Rey, P.; Subra, R.; Schweizer, J. *J. Am. Chem. Soc.* **1994**, *116*, 2019.

(30) Zheludev, A.; Grand, A.; Ressouche, E.; Schweizer, J.; Morin, B. G.; Epstein, A. J.; Dixon, D. A.; Miller, J. S. *J. Am. Chem. Soc.* **1994**, *116*, 7243.

(31) Zheludev, A.; Bonnet, M.; Delley, B.; Grand, A.; Luneau, D.; Öhrström, L.; Ressouche, E.; Rey, P.; Schweizer, J. *J. Magn. Magn. Mater.* **1995**, *140–144*, 1441.

(32) Andzelm, J.; Wimmer, E. *J. Chem. Phys.* **1992**, *96*, 1280.

(33) UniChem 2.3; Cray Research, Inc.: 2360 Pilot Knob Road, Mendota Heights, MN 55120, 1994.

(34) Vosko, S. H.; Wilk, L.; Nusair, M. *Can. J. Phys.* **1980**, *58*, 1200.

(35) (a) Becke, A. D. *Phys. Rev. A* **1988**, *38*, 3098. (b) Perdew, J. P. *Phys. Rev. B* **1986**, *33*, 8822.

(36) Godbout, N.; Salahub, D. R.; Andzelm, J.; Wimmer, E. *Can. J. Chem.* **1992**, *70*, 560.

(37) Chen, H.; Krasowski, M.; Fitzgerald, G. J. *J. Chem. Phys.* **1993**, *98*, 8710.

(38) Norrby, P.-O.; Kolb, H. C.; Sharpless, K. B. *Organometallics* **1994**, *13*, 344.

(39) Fan, L.; Ziegler, T. *J. Chem. Phys.* **1991**, *94*, 6057.

(40) Fukushima, N.; Waizumi, K. *Chem. Express* **1993**, *8*, 265.

(41) (a) Noodleman, L.; Case, D. A. *Adv. Inorg. Chem.* **1992**, *38*, 423. (b) Mouesca, J.-M.; Chen, J. L.; Noodleman, L.; Bashford, D.; Case, D. A. *J. Am. Chem. Soc.* **1994**, *116*, 1898.

can be expressed as:

$$E(S_{\max} = S_{\text{Cu}} + S_{\text{Mn}}) - E(M_S = S_{\text{Mn}} - S_{\text{Cu}}) = E_{\text{HS}} - E_{\text{BS}} = 2JS_{\text{Mn}}S_{\text{Cu}} = 5J/2 \quad (1)$$

The spin populations were corrected in the following way:^{42,43}

$$p_M = \frac{K_M p_{\text{BS}} S}{S_M} \quad (M = \text{Mn, Cu})$$

$$K_{\text{Mn}} = \frac{S(S+1) + [S_{\text{Mn}}(S_{\text{Mn}}+1) - S_{\text{Cu}}(S_{\text{Cu}}+1)]}{2S(S+1)}$$

$$K_{\text{Cu}} = \frac{S(S+1) - [S_{\text{Mn}}(S_{\text{Mn}}+1) - S_{\text{Cu}}(S_{\text{Cu}}+1)]}{2S(S+1)} \quad (2)$$

where p_{BS} is the calculated spin population for the BS state, p_M is the corrected spin population for the metal or its nearest neighbors in the $S = 2$ ground state, and S_M is the local spin for $M = \text{Mn(II)}$ or Cu(II) . Thus, the spin populations were multiplied by 4/6 for Cu(II) and its neighbors, and by $^{28}/_{30}$ for Mn(II) and its neighbors. It is worth noticing that, if the spins were entirely localized on the metal ions, this correction would give the populations $+4.67 \mu_B$ (Bohr magneton) and $-0.67 \mu_B$ on Mn(II) and Cu(II) , respectively, which corresponds to the Heitler–London solution (see below).

In addition, another implementation of the DFT method, the DMol program (version 2.3.7),⁴⁴ was tested. The standard DND basis set was utilized. It includes a double numeric basis set for all valence electrons plus one d-polarization function for C, N, and O atoms. This basis set is thought to be appropriate for coordination complexes. Metal f-polarization functions have been found to be of minor importance for such species. Charge and spin densities were cast by partitioning and projection into a multipolar basis set free representation up to $L = 3$ ($L = 2$ for hydrogen) for efficient calculation of the Kohn–Sham potential.⁴⁴

The geometries of the model compounds were taken from the neutron diffraction study.

Polarized Neutron Diffraction and Spin-Density Maps

Principles. Diffraction of a neutron beam by a magnetically ordered single crystal gives rise to Bragg reflections of scattering vector \mathbf{k} , the intensities $I(\mathbf{k})$ of which depend on both nuclear $F_{\text{N}}(\mathbf{k})$ and magnetic $F_{\text{M}}(\mathbf{k})$ structure factors. In the case of a paramagnetic compound a strong magnetic field is applied in order to align the electronic unpaired spins in the sample. Polarized neutron diffraction is now a well-established technique to determine weak magnetic structure factors.⁴⁵ The experimental magnetic structure factors can be directly derived from the measured flipping ratios in the case of a centrosymmetrical cell, knowing the nuclear structure factors. This is the reason why a precise structure determination must be undertaken in complement to the polarized neutron study, the two experiments being performed in the same temperature range.

In the case of hydrogen-containing compounds as in the present study, a correction must be applied in order to take into account the polarization of the hydrogen nuclei by the strong magnetic field at low temperature, which gives rise to a contribution to the diffracted intensity. The corresponding nuclear polarization structure factor is written as:

$$F_{\text{NP}}(\mathbf{k}) = \sum_i f_{\text{NP}}^i \exp(i\mathbf{k}\mathbf{r}_i) \exp(-W_i) \quad (3)$$

where f_{NP}^i is the hydrogen spin polarization at a given temperature and field, \mathbf{r}_i is the vector defining the position of hydrogen i with respect to the origin of the cell, and W_i is the Debye–Waller factor associated with this hydrogen i .

The spin distribution can then be derived from an experimental F_{M} 's data set, either by direct methods like Fourier summation or maximum entropy method,⁴⁶ or alternatively by indirect methods via a modeling of the spin density based on a molecular orbital model^{47–49} or a multipole model.^{23,50,51}

Data Analysis and Results. The experimental spin-density map was obtained by refining a multipole model on the basis of the experimental magnetic structure factors. The model has been widely applied to spin-distribution studies for organic radicals.^{23,29} and transition metal complexes.^{25,26,52} In this model the density is written as a sum of atomic densities, each of them being a linear combination of multipolar functions $\rho_{\text{lm}}(\mathbf{r}_i)$ with population coefficients P_{lm}^i .⁵³

The exact analogy between the multipole expansion and the development of the spin density on the basis of atomic orbitals has been established in the case of a 3d single-electron system.⁵⁴

In the wavefunction approach the spin density of a molecule is approximated by the sum of atomic spin densities:

$$\rho(\mathbf{r}) = \sum_i p_i \rho_i(\mathbf{r}_i) \quad (4)$$

where p_i is the spin population of the atom i .

The program used to refine the spin density²³ was originally derived from the program MOLLY devoted to charge density.⁵⁰ This program was recently modified in order to refine atomic orbital populations, using restraints taking into account the relationships between multipole populations p_{lm}^i and orbital populations.⁵²

The Slater radial exponents ζ together with the n_l values, given in Table 3, were deduced from atomic Slater exponents ξ taken from the literature,^{55,56} using the relation $\zeta = 2\xi$.

Two scaling factors were refined with the three data sets. The manganese spin distribution was described by a spherical multipolar function assuming equal populations in the five 3d orbitals. This assumption of equal populations is valid only in a crystal-field approximation where the electronic delocalization within the $t_{2g}^3 e_g^2$ configuration is ignored. Simple monopoles were considered for the carbon, nitrogen, and oxygen atoms, this assumption being justified by the very weak spin populations carried by these atoms. It was not possible from the data to refine the shape of the spin density around the copper atom, and therefore a constraint was applied to the multipoles centered on this atom: It was assumed that the unpaired electron arising from the Cu(II) ion was described by a xy -type orbital, the x axis running along the Mn–Cu direction, and the y axis being

(46) Papoular, R.; Gillon, B. *Europhys. Lett.* **1990**, *13*, 429.

(47) Wedgwood, F. A.; *Proc. R. Soc. London* **1976**, *A349*, 447.

(48) Figgis, B. N.; Mason, R.; Smith, A. R. P.; Williams, G. A. *J. Am. Chem. Soc.* **1979**, *101*, 3673.

(49) Figgis, B. N.; Kucharski, E. S.; Vrtis, M. *J. Am. Chem. Soc.* **1993**, *115*, 176.

(50) Mason, R.; Smith, A. R. P.; Varghese, J. N.; Chandler, G. S.; Figgis, B. N.; Phillips, R. A.; Williams, G. A. *J. Am. Chem. Soc.* **1981**, *103*, 1300.

(51) Brown, P. J.; Capiomont, A.; Gillon, B.; Schweizer, J. *Mol. Phys.* **1983**, *48*, 753.

(52) Ressouche, E.; Boucherle, J. X.; Gillon, B.; Rey, P.; Schweizer, J. *J. Am. Chem. Soc.* **1993**, *115*, 3610.

(53) Hansen, N. K.; Coppens, P. *Acta Crystallogr.* **1978**, *A34*, 909.

(54) Holladay, A.; Leung, P.; Coppens, P. *Acta Crystallogr.* **1953**, *A39*, 377.

(55) Clementi, E.; Raimondi, D. L. *J. Chem. Phys.* **1963**, *38*, 2686.

(56) Hehre, W. J.; Stewart, R. F.; Pople, J. A. *J. Chem. Phys.* **1969**, *51*, 2657.

(42) McWeeny, R.; Sutcliffe, B. T. *Methods of Molecular Quantum Mechanics*; Academic Press: London, 1969; p 104.

(43) Mouesca, J.-M.; Rius, G.; Lamotte, B. *J. Am. Chem. Soc.* **1993**, *115*, 4714.

(44) (a) Delley, B. *J. Chem. Phys.* **1990**, *92*, 508. (b) Perdew, J. P.; Wang, Y. *Phys. Rev. B* **1992**, *45*, 13244.

(45) Brown, P. J.; Forsyth, J. B.; Mason, R. *Phil. Trans. R. Soc. London* **1980**, *B290*, 481.

Table 3. Model Refinements: Reliability Factors, Radial Coefficients, and Spin Populations (in μ_B) Normalized to $4 \mu_B^a$

Refinement Conditions and Reliability Factors			
no. of reflns	332		
refinement no.	I	II	
no. of parameters	18	14	
$R_w(F)$	0.065	0.066	
χ^2	2.7	2.7	
m_l Indexes and Slater Exponents ζ (ua^{-1})			
		ζ	
	m_l	I	II
Mn	4	6.82(5)	6.81(5)
Cu	4	8.8(6)	9.6(6)
O	2	4.5	4.5
N	2	3.9	3.9
C	2	3.44	3.44
Spin Populations (in μ_B)			
		I	II
Mn		4.39(2)	4.32(2)
Cu		-0.48(1)	-0.47(1)
O1		0.02(1)	0.03(1)
O2		0.02(1)	0.03(1)
N5		0.10(1)	0.09(1)
N6		0.08(1)	0.08(1)
N7		0.08(1)	0.07(1)
N8		0.06(1)	0.05(1)
N1		-0.06(1)	-0.05(1)
N2		-0.06(1)	-0.05(1)
N3		-0.03(1)	-0.02(1)
N4		-0.05(1)	-0.02(1)
C1		-0.01(2)	-0.03(1)
C2		-0.07(2)	-0.03(1)

^a $R_w(F) = \{\sum_{hkl}[\sigma^{-1}(F_c - F_o)]^2\} / \{\sum_{hkl}(F_o/\sigma)^2\}$; $\chi^2 = \{\sum_{hkl}[\sigma^{-1}(F_c - F_o)]^2\} / \{N_o - N_v\}$, with N_o = number of reflections and N_v = number of parameters.

situated within the plane of the bridging network. This restraint corresponds to the following relationships between the quadrupole P_{20} and hexadecapole P_{40} populations on the one hand, and the refined monopole P_{00} population on the other hand:⁵⁷

$$\begin{aligned}
 P_{20} &= -0.274929P_{00} \\
 P_{40} &= 0.061413P_{00} \\
 P_{44} &= -(1/\pi)P_{00}
 \end{aligned}
 \quad (5)$$

Moreover, the P_{00} populations of the non-metal atoms were constrained to take into account the presence of a quasi-mirror plane (zx) containing the metal atoms and perpendicular to the oxamido bridge. The quality of refinement II is practically the same as that of the purely spherical refinement I, as shown in Table 3.

The sum of the monopole populations obtained from refinement II before normalization provides a value of $3.65(15) \mu_B$ for the induced moment per molecule, which has to be compared with the measured magnetization equal to $3.93 \mu_B$ at 2 K under 50 kOe. The spin populations as given by the monopole populations normalized to a moment of $4 \mu_B$ are reported in Table 3.

The spin-density maps in projection along the perpendicular to the plane of the bridging network and along the perpendicular to the N6-Mn-Cu plane are presented in Figures 3 and 4, respectively. Positive spin populations are observed on the atoms belonging to the manganese coordination sphere while negative spin populations are observed on the nitrogen atoms

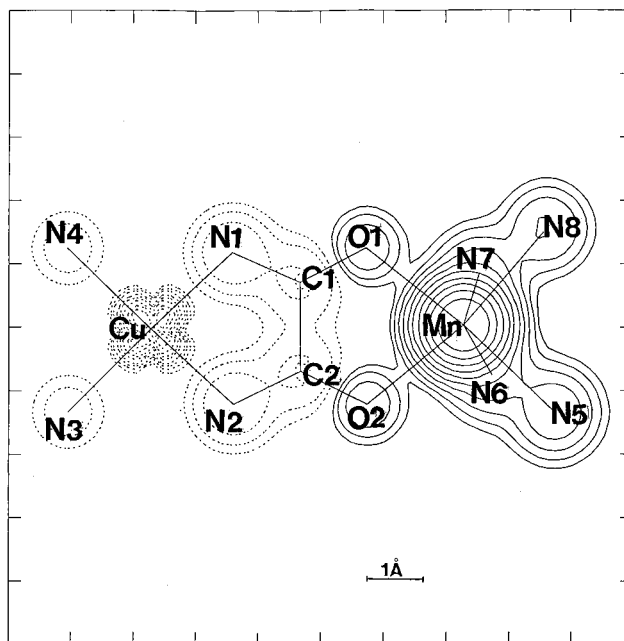


Figure 3. Spin-density map for MnCu at 2 K under 50 kOe in projection along the perpendicular to the oxamido mean plane. Solid lines are used for positive and dashed lines for negative spin densities. Contours are $\pm 0.005 \times 2^{n-1} \mu_B$, with $n = 1, 2, \dots$

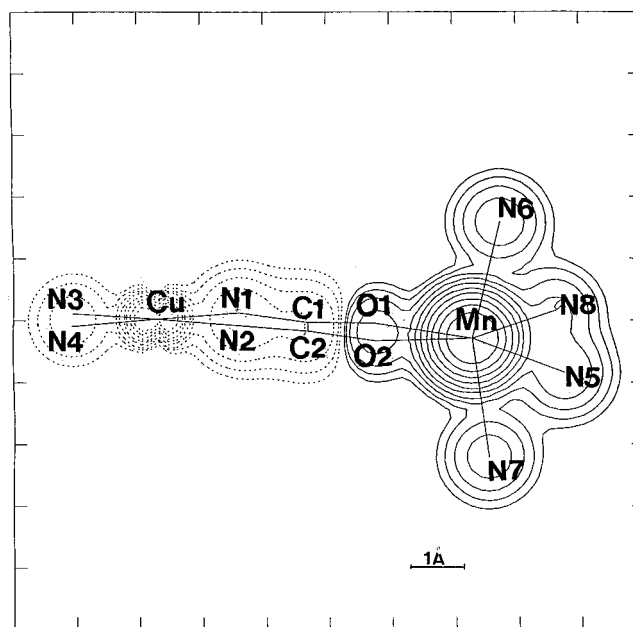
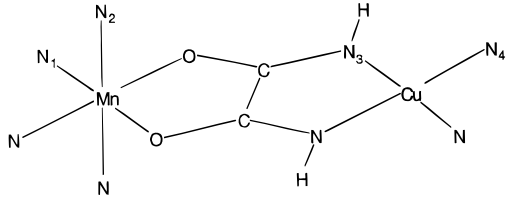


Figure 4. Spin-density map for MnCu at 2 K under 50 kOe in projection along the perpendicular to the N6-Mn-Cu plane.

surrounding the copper atom. The spin populations on the carbon, nitrogen, and oxygen atoms only amount a few hundredths of μ_B , and therefore cannot be considered as being entirely reliable. The spin populations on the light atoms given in Table 3, however, may be considered as a trend. The spin population transferred from the Mn(II) ion to the oxygen atoms of the bridge [mean value $0.03(1) \mu_B$ per oxygen atom] is twice as small as the spin amount transferred toward the nitrogen atoms of the tetradentate terminal ligand [mean value $0.07(1) \mu_B$ per nitrogen atom]. The spin delocalization is more pronounced toward the nitrogen than the oxygen atoms linked to the manganese atom although the Mn-N bond length [mean value $2.30(2) \text{ \AA}$] is significantly longer than the Mn-O bond length [mean value $2.16(2) \text{ \AA}$]. The spin populations on the bridging nitrogen atoms linked to the copper atom are equal to $-0.05(1) \mu_B$ while those on the peripheral nitrogen atoms of

(57) Ressouche, E. PhD Thesis, Université de Grenoble, 1991.

Table 4. Atomic Spin Populations (in μ_B) Calculated in the Heitler–London (H.L.) and Heitler–London + Spin Delocalization Extended–Hückel Formalism (H.L. + E.H.) Approaches for the Model Molecule Shown Below (See Text)



atom	H.L.	H.L. + E.J.
Mn	4.67	4.475
Cu	-0.67	-0.360
O		0.055
N ₁		0.015
N ₂		0.017
N ₃ + H		-0.124
N ₄		-0.020
C		-0.001

the copper coordination sphere are equal to $-0.02(1) \mu_B$. Finally, weak negative spin populations ($-0.03(1) \mu_B$) on the carbon atoms of the oxamido bridge have been found. The sum of the positive and negative spin populations is equal to $+4.67 \mu_B$ and $-0.67 \mu_B$, respectively, which exactly corresponds to what is predicted by the Heitler–London description of the $S = 2$ ground state (see below).

A striking result emerges from the spin-density maps of Figures 3 and 4. Even though the positive spin density on the manganese side is much larger in absolute value than the negative spin density on the copper side, the nodal surface of zero spin density is closer to the manganese atom than to the copper one. This nodal surface intersects the Mn–Cu direction at a point located 2.18 Å from Mn and 3.25 Å from Cu.

Theoretical Study. Heitler–London + Extended Hückel Approach

In this section and the following one we will discuss the results in terms of atomic spin populations using different approaches, of increasing complexity.

Spin Coupling. The simplest description of the $S = 2$ ground state consists of coupling the $S_{Mn} = 5/2$ and $S_{Cu} = 1/2$ local spins. Such a description leads to the eigenfunction $|2,2\rangle$ for the $M_S = 2$ Zeeman component of the quintet state:

$$|2,2\rangle = \sqrt{\frac{5}{6}}|5/2,5/2\rangle|1/2,-1/2\rangle - \sqrt{\frac{1}{6}}|5/2,3/2\rangle|1/2,1/2\rangle \quad (6)$$

where the kets in the right-hand side of eq 6 stand for $|S_{Mn}, M_{S_{Mn}}\rangle$ and $|S_{Cu}, M_{S_{Cu}}\rangle$. The eigenfunction in eq 6 leads to the spin populations on the Mn(II) and Cu(II) ions:

$$\begin{aligned} p_{Mn} &= 7g_2/3 \\ p_{Cu} &= -g_2/3 \end{aligned} \quad (7)$$

where g_2 is the Zeeman factor for the $S = 2$ ground state, found as 1.978 from the fitting of the magnetic susceptibility data.²⁶ In the following, we will take $g_2 = 2$ for the sake of simplicity, which gives $p_{Mn} = 4.67 \mu_B$ and $p_{Cu} = -0.67 \mu_B$ (see the first column of Table 4). The fact that p_{Mn} and p_{Cu} are not equal to $5 \mu_B$ and $-1 \mu_B$, respectively, comes from the fact that the ground state is not strictly a Neel state with antiparallel $S_{Mn} = 5/2$ and $S_{Cu} = 1/2$ spins. In addition to the dominant $|5/2,5/2\rangle$

$2 > |1/2, -1/2\rangle$ contribution, the eigenfunction contains a weak $|5/2,3/2\rangle|1/2,1/2\rangle$ contribution.

Spin Delocalization. A better description of the ground state may be obtained in taking into account the delocalization of the magnetic orbitals from the metal on which they are centered toward the ligands linked to this metal. Let us define by a_μ , $\mu = 1-5$, the five magnetic orbitals centered on Mn(II), and by b the unique magnetic orbital centered on Cu(II). The $M_S = 2$ Zeeman component of the $S = 2$ ground state then becomes:

$$\begin{aligned} \Psi(S=2, M_S=2) &= \sqrt{\frac{5}{6}}(a_1 a_2 a_3 a_4 a_5 \bar{b}) - \\ &\sqrt{\frac{1}{30}}[(\bar{a}_1 a_2 a_3 a_4 a_5 b) + (a_1 \bar{a}_2 a_3 a_4 a_5 b) + (a_1 a_2 \bar{a}_3 a_4 a_5 b) + \\ &(a_1 a_2 a_3 \bar{a}_4 a_5 b) + (a_1 a_2 a_3 a_4 \bar{a}_5 b)] \quad (8) \end{aligned}$$

The delocalization of the magnetic orbitals may be quantitatively estimated, using the orbital contraction method, in the extended Hückel formalism. Such a method was already utilized in the case of the Cu(salen)Ni(hfa)₂ compound.²⁶ Let us recall briefly what is its philosophy. The five magnetic orbitals a_μ may be considered as the singly-occupied orbitals for the $S_{Mn} = 5/2$ local state of the Mn(II) ion in MnCu. Similarly, b may be considered as the singly-occupied orbital for the $S_{Cu} = 1/2$ local state of the Cu(II) ion in MnCu. In other terms, the magnetic orbitals describe the unpaired electrons at the zeroth order, when the interaction between the magnetic centers is ignored. It follows that the a_μ 's can be determined in considering the compound MnCu as a whole, with its actual geometry, but in contracting the Cu atomic orbitals in a way to prevent any orbital interaction between the copper atom and its surroundings. In the same way, b can be determined in contracting the Mn atomic orbitals, in order to prevent any orbital interaction between the manganese atom and its surroundings. The $p_{a_\mu,i}$ spin populations on the atom i in the orbital a_μ , and $p_{b,i}$ electronic populations on the atom i in the orbital b were then calculated using the extended Hückel formalism. The spin populations p_i on the atom i , expressed in Bohr magneton, are then given by:

$$p_i = g_2 \left[\frac{7}{15}(p_{a_1,i} + p_{a_2,i} + p_{a_3,i} + p_{a_4,i} + p_{a_5,i}) - \frac{1}{3}p_{b,i} \right] \quad (9)$$

The atomic spin populations obtained in this way are given in Table 4.

Theoretical Study. Density Functional Theory Approach

We will successively determine the spin populations for monomeric fragments, the spin populations, and spin densities for the actual MnCu compound, and finally calculate the energy gap between low-lying states in MnCu.

Spin Populations in Mononuclear Fragments. For the first time, we considered the three mononuclear fragments, 1–3, shown below:

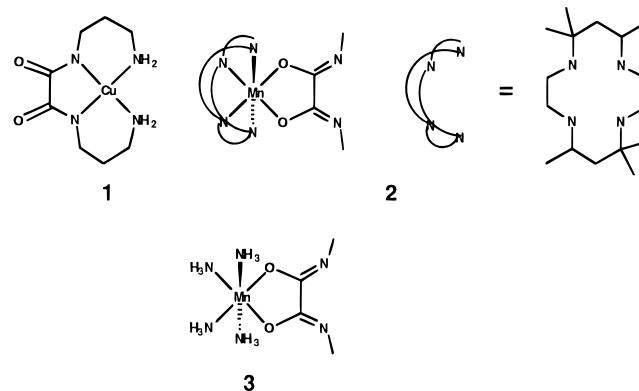


Table 5. Mulliken Spin Populations (in μ_B) for Model Compounds 1–4. Values in Italics Are Populations with Mostly π -Character, All Others Are Mainly of σ -Type (in the xy Plane)

	1	2	3	4	4	4
spin state	1/2	5/2	5/2	3	BS	$\sim 2^a$
Mn		4.66	4.64	4.79	4.72	4.41
NH ₃ ax ^b		0.02	0.03	0.03	0.03	0.03
NH ₃ seq ^b		0.01	0.02	0.03	0.02	0.02
O	0.09	0.08	0.08	0.04	0.02	0.02 ^c
C	-0.01	-0.01	-0.01	-0.01	0.00	0.00 ^c
N	0.15	0.05	0.05	0.16	-0.12	-0.08 ^c
Cu	0.38			0.44	-0.41	-0.27
NH ₂ ^b	0.06			0.10	-0.09	-0.06

^a The correct broken symmetry (BS) state populations (see text).

^b Including hydrogen populations. ^c Due to contribution from both metal ions, the corrections for the bridge are only approximative.

with a somewhat idealized geometry. The fragment **1** actually does exist; it is the neutral copper(II) precursor used to synthesize MnCu. The structure of fragment **2** was taken from the neutron diffraction study, as was **1**, while for **3** the positions of the coordinating nitrogen atoms were retained, but the macrocycle Me₆-[14]ane-N₄ was replaced by four NH₃ molecules.

The spin populations are given in Table 5. This table reveals a large difference as for the behavior of the metal ions. The Mn(II) ion in **2** carries 93% of its formal spin population, while Cu(II) in **1** extensively shares its spin density with the surrounding ligands, and retains only 38% of the unpaired electron. This is in agreement with the fact that Mn(II) prefers electrostatic bonds, while the many d electrons of Cu(II) make it prone to more covalent bonds.⁵⁸ Furthermore, for **1**, a negative spin polarization of the π orbitals of the oxamido carbon atoms is found, which may be attributed to the same mechanism as that producing the negative spin population on the hydrogen atoms of the methyl radical.⁵⁹ The formation of molecular orbitals (MO) involving d metal and σ ligand atomic orbitals transfers some spin density of σ symmetry to the nitrogen or oxygen atoms. The π bond is then polarized, with a small fraction pairing up with the positive density on the nitrogen or oxygen atoms, leaving a negative fraction on the carbon atoms.

The situation is a bit more complicated for fragments **2** and **3**. A large positive density on the oxamido nitrogen atoms is observed, which cannot be explained by a spin-polarization effect. We are likely faced with the effect of an occupied π orbital donating a fraction of the β spin electron to the empty d metal orbitals, thus leaving a small net positive density in the original MO. These π orbitals produce another kind of spin polarization, similar to what occurs in the allyl radical,⁶⁰ with a negative spin density induced on the nodal (or with small MO coefficients) atoms. Thus, a large coefficient on the oxygen atoms and a node (or much smaller coefficients) on the carbon atoms may also explain the negative spin density on these carbon atoms (see Figure 5c).

We can thus identify three different mechanisms for the transfer of spin from either of the metal ions to the oxamido bridge. Neither of them can be quantified, but since the role of spin polarization on magnetic interaction has recently been debated,^{61,62} we would like to discuss their different influences in this respect.

(58) Greenwood, N. N.; Earnshaw, A. *Chemistry of the Elements*; Pergamon Press: Oxford, 1984.

(59) Borden, W. T. *Modern Molecular Orbital Theory for Organic Chemists*; Prentice-Hall: Englewood Cliffs, NJ, 1975.

(60) See, for instance: Altherton, N. M. *Principles of Electron Spin Resonance*; Ellis Horwood-Prentice Hall: London, 1993; pp 90–108;

(61) Kollmar, C.; Kahn, O. *Acc. Chem. Res.* **1993**, *26*, 259.

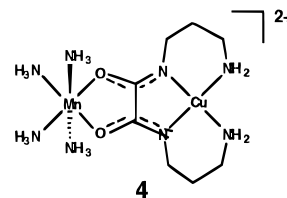
(62) Miller, J. S.; Epstein, A. J. *Angew. Chem., Int. Ed. Engl.* **1994**, *33*, 385.

(i) **Spin Delocalization from Cu(II) and Mn(II) through the σ Bonds.** This should favor an antiferromagnetic interaction since the extension of the d-type magnetic orbitals brings the spin densities closer to each other (see Figure 5d).

(ii) **Spin Delocalization from the Oxamido π Orbitals to the Mn(II) Empty d Orbitals.** This interaction is responsible for the spin density in the π orbital of the oxamido nitrogen atom of fragments **2** and **3**. This effect, combined with the first mechanism, is ferromagnetic in nature, since it puts spin density in orthogonal atomic orbitals on the same atom (the oxamido nitrogen atom bonded to Cu) (see Figure 5e).

(iii) **Spin Polarization of the Bridge.** In order to know whether this is a ferro- or an antiferromagnetic contribution, we have to realize that the spin polarization originates from the orthogonal orbitals on the nitrogen and oxygen atoms. If the spin densities on the two metal ions have different signs, then this favors a local ferromagnetic interaction on nitrogen and oxygen atoms while retaining the spins paired on the carbon atoms. Therefore, this interaction should be antiferromagnetic (see Figure 5f).

Spin Populations and Spin Densities in MnCu. The calculations were performed for the $S = 3$, BS, and $S = 2$ states of MnCu with the simplified geometry **4** where the tetradentate ligand on the manganese was replaced by four NH₃ molecules.



The BS spin populations were then corrected to the $S = 2$ ground state, as indicated above. The orbital energy diagrams are shown in Figure 6. The spin populations are reported in Table 5.

For the three states the calculated spin density is found to be essentially spherical on Mn(II), and to have the xy -symmetry on Cu(II). We also see that although the mononuclear fragments **1** and **2** (or **3**) can give valuable clues concerning the orbital interactions, the spin population in the $S = 3$ state of **4** is not the simple sum of the spin populations on the fragments. For example, on the manganese side a redistribution of the unpaired electron toward the NH₃ ligands takes place (see Table 5). The DGauss and DMol results are almost identical, as shown in Table 6.

It would be somewhat cumbersome to compare in detail the calculated and experimental spin populations given in Table 6. Indeed, we must keep in mind the approximations of the calculation method. For instance, the spin populations on the oxamido bridge have contributions arising from both metal ions, thus making the correction from the BS to the $S = 2$ state only approximative. Moreover, strictly speaking, the experimental and theoretical values of Table 6 are not comparable. They represent population analyses for different kinds of basis functions with different spatial distributions, so that we cannot expect a perfect agreement between the different methods of spin density reconstruction. A striking feature, however, emerges from Table 6, namely the discrepancy between the calculated and observed spin populations on Cu(II), $-0.47 \mu_B$ (exp) vs $-0.27 \mu_B$ (calc). The same type of discrepancy has already been observed in some copper–nitronyl nitroxide compounds.⁶³ Figure 7 shows the DMol spin density map for the BS state, which may be compared to the experimental spin density map of Figure 3. A close look at Figure 7 reveals that

(63) Öhrström, L.; Grand, A.; Pey, P. Unpublished results.

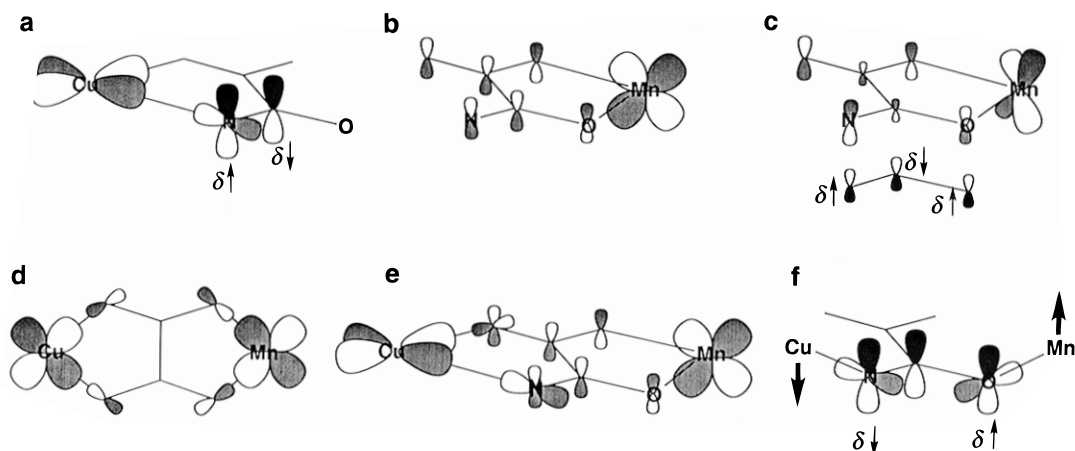


Figure 5. Mechanisms of spin transfer toward the bridges. (a) The donation of α and β spin density from the bridge toward the singly occupied d_{xy} copper orbital leaves an excess of α spin density on the bridge. (b) Interaction with a manganese d_{xz} orbital. The π orbital on the bridge in this case has a very small coefficient on the carbon atoms, and thus an underlying π orbital will be polarized. (c) All the π orbitals have roughly the same weight, so that there will be no resulting spin polarization. (d) Spin delocalization from Cu(II) and Mn(II) through the σ -bonds. (e) Spin delocalization from the oxamido π orbitals to the Mn(II) empty d orbitals. (f) Spin polarization of the bridge (see text).

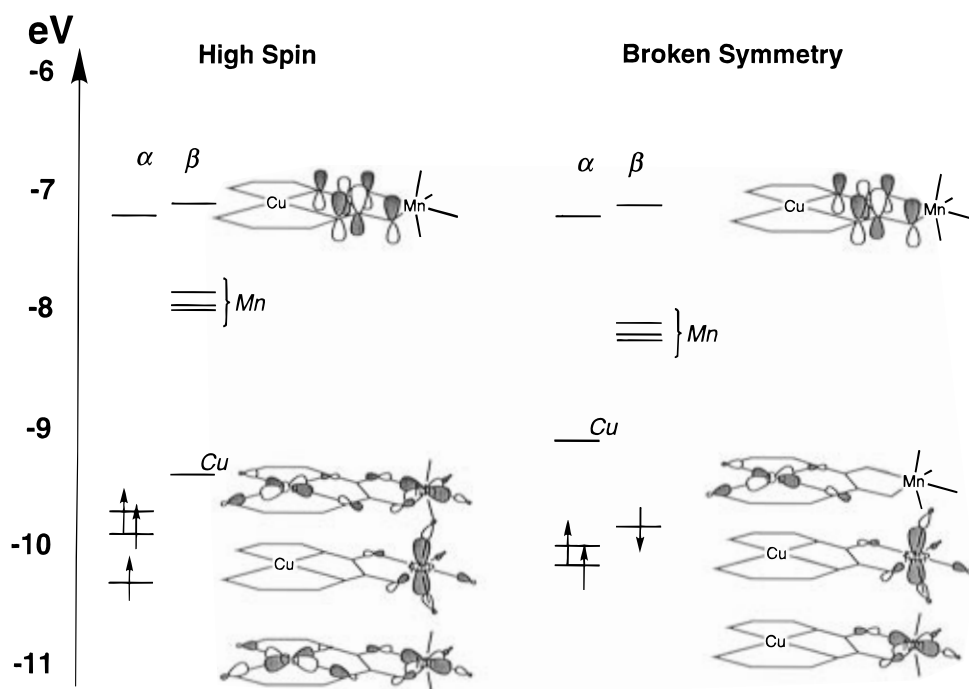


Figure 6. Orbital energy diagram for the $S = 3$ and broken symmetry (BS) states of the model compound **4**. The principal character of the three highest occupied metal orbitals and the σ and π^* orbitals of the bridge are also indicated.

Table 6. Experimental and Calculated Mulliken Spin populations (in μ_B) for Model Compound **4**

	neutrons	H.L.	H.L. + E.H.	DMol	DGauss	DGauss
spin state		2	2	BS	BS	$\sim 2^a$
Mn	4.32(2)	4.67	4.47	4.68	4.72	4.41
NH ₃ ax ^b	0.07(1)		0.02	0.03	0.03	0.03
NH ₃ eq ^b	0.07(1)		0.02	0.02	0.02	0.02
O	0.03(1)		0.05	0.01	0.02	0.02 ^c
C	-0.03(1)		0.00	0.01	0.00	0.00 ^c
N	-0.05(1)		-0.12	-0.11	-0.12	-0.08 ^c
Cu	-0.47(1)	-0.67	-0.36	-0.42	-0.41	-0.27
NH ₂ ^b	-0.02(1)		-0.02	-0.09	-0.09	-0.06

^{a-c} As in Table 5.

the nitrogen populations are heavily polarized in the direction of the metal. We then suggest that the division of the spin density between nitrogen and copper contributions is not straightforward, neither in the calculations nor in the treatment of the experimental data. The two approaches clearly use different criteria, and then of course end up with different

answers. If we instead sum the contributions of the copper and its nearest neighbor atoms, we get a much more coherent picture, $-0.61 \mu_B$ (exp) versus $-0.55 \mu_B$ (calc). The same may hold for the manganese side where the calculated spin populations on the nitrogen atoms are lower than the experimental ones. Here, we have also to take into account the fact that the macrocycle has been replaced by NH₃ molecules. It clearly appears in Table 5 that the NH₃ molecules are less polarized.

The discrepancy concerning the oxamido carbon atoms is less disturbing. Indeed, in the bridging region there is no possibility of making a correction from the BS to the $S = 2$ state. We can notice, however, that our calculation suggests a viable mechanism for the negative spin density on these atoms.

Quintet–Septet Energy Gap for MnCu. The accurate calculation of the energy gaps between low-lying states in polymetallic compounds is a difficult problem. The classical study by de Loth et al. on copper(II) acetate points out the formidable task of bringing theory in agreement with experi-

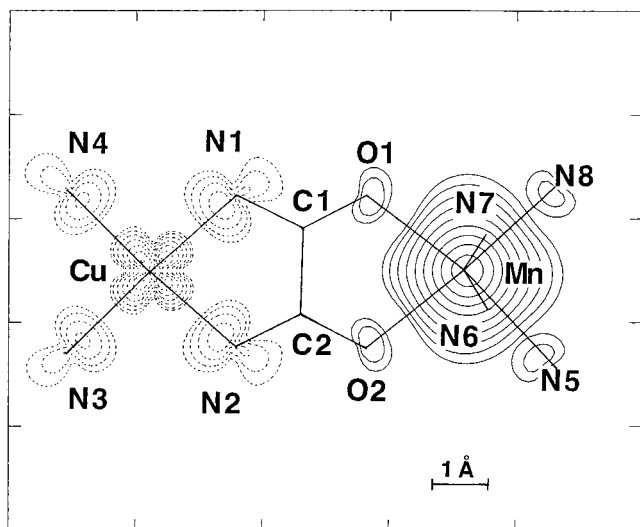


Figure 7. Calculated spin-density map for the broken symmetry (BS) state of the model compound **4** in projection along the perpendicular to the oxamido mean plane. The contours are the same as in Figure 3, so that those two figures may be compared.

ment.⁶⁴ Recently, CASSCF and multireference CI calculations on binuclear Ti(III), V(III), and Cr(III) oxo-bridged species were reported.⁶⁵ In the present case the calculated value of the ground quintet–excited septet energy gap is $3J = -710 \text{ cm}^{-1}$ using the DGauss program, and -806 cm^{-1} using the DMol program, which in both cases is much larger than the experimental value of -93.3 cm^{-1} . This discrepancy between calculated and experimental energy gap may seem to be rather large, but in quantum chemical terms 600 cm^{-1} (1.7 kcal) is a small quantity. Less pronounced discrepancies have been found in other DFT calculations with BS states.⁶⁶ In the present case, the large error is probably due to the use of a smaller basis set for copper, double- ζ instead of triple- ζ . The predictive value of this type of calculation is of course limited, but it was nevertheless interesting to test the performance of simple and straightforward computations, relative to elaborate CASSCF and CI schemes.

Conclusion

The heterobimetallic compounds have played a crucial role in the field of molecular-based magnets. A better understanding of the electronic structure of these compounds requires the knowledge of the spin distribution in the ground state. This paper reports on the spin distribution in the $S = 2$ ground state of an antiferromagnetically coupled Mn(II)Cu(II) pair, determined from both polarized neutron diffraction data and theoretical computations.

(64) de Loth, P.; Cassoux, P.; Daudey, J. P.; Malrieu, J. P. *J. Am. Chem. Soc.* **1981**, *103*, 4007.

(65) Fink, K.; Fink, R.; Staemmler, V. *Inorg. Chem.* **1994**, *33*, 6219.

(66) Noodleman, L.; Case, D. A.; Aizman, A. *J. Am. Chem. Soc.* **1988**, *110*, 1001.

Concerning the experimental results, the main findings may be summed up as follows: In the $S = 2$ ground state of MnCu large positive and weak negative spin densities are found in the vicinity of the manganese and copper atoms, respectively. Both the positive and negative spin densities are delocalized from the metal centers toward the terminal and bridging atoms surrounding these metal centers. The negative spin density arising from copper is much weaker in absolute value than the positive spin density arising from manganese. However, this negative spin density is more delocalized than the positive one, and the nodal surface between positive and negative spin density regions is closer to the manganese than to the copper atom. The carbon atoms of the oxamido bridge carry a weak negative spin density. From a quantitative point of view, the sum of the positive atomic spin populations is equal to $4.67 \mu_B$, and the sum of the negative atomic spin populations is equal to $-0.67 \mu_B$. These values exactly correspond to what is predicted by a Heitler–London description of the $S = 2$ ground state. This agreement confirms, if it was still necessary, the quality of such a description of the low-lying states of coupled systems.¹

The data deduced from polarized neutron diffraction have been compared to theoretical data obtained through different computational methods. The simplest approach consisted of introducing the spin delocalization in the Heitler–London scheme, using the concept of magnetic orbitals in the extended Hückel formalism. Such an approach leads to spin populations which compare fairly well to the experimental data. The main limitation of this approach, however, is that it totally ignores the spin polarization effects. In a second experiment, two types of density functional theory (DFT) calculations were performed, which again reproduce the spin density map in a satisfying way, and provide new insights on both spin delocalization and spin polarization effects. The main difference between experimentally determined and calculated spin populations concerns the distribution of the spin density between the copper atom and the nitrogen atoms linked to copper. The spin populations are evidently not physical observables. The decomposition of the spin density in atomic spin populations depends on some rather arbitrary criteria which are not strictly the same for the interpretation of the experimental and theoretical data.

A heterobinuclear compound such as that investigated in this work represents the simplest case of a Mn(II)Cu(II) system. In a future work we will report on the spin-density map of a Mn(II)Cu(II) ferrimagnetic chain compound.

Acknowledgment. We thank the Commissariat à l’Energie Atomique (CEA) for the use of the CRAY-C94 supercomputer in Grenoble. L.Ö. gratefully acknowledges a postdoctoral fellowship from the Swedish Research Council for Engineering Sciences and the Swedish Institute for funding. Dr. J. M. Mouesca is thanked for valuable discussions.

JA961545P